
Motion Adaptation Leads to Parsimonious Encoding of Natural Optic Flow by Blowfly Motion Vision System

J. Heitwerth,¹ R. Kern,¹ J. H. van Hateren,² and M. Egelhaaf¹

¹Department of Neurobiology, Faculty for Biology, Bielefeld University, Bielefeld, Germany; and ²Department of Neurobiophysics, University of Groningen, Groningen, The Netherlands

Submitted 23 March 2005; accepted in final form 18 May 2005

Heitwerth, J., R. Kern, J. H. van Hateren, and M. Egelhaaf. Motion adaptation leads to parsimonious encoding of natural optic flow by blowfly motion vision system. *J Neurophysiol* 94: 1761–1769, 2005. First published May 25, 2005; doi:10.1152/jn.00308.2005. Neurons sensitive to visual motion change their response properties during prolonged motion stimulation. These changes have been interpreted as adaptive and were concluded, for instance, to adjust the sensitivity of the visual motion pathway to velocity changes or to increase the reliability of encoding of motion information. These conclusions are based on experiments with experimenter-designed motion stimuli that differ substantially with respect to their dynamical properties from the optic flow an animal experiences during normal behavior. We analyze for the first time motion adaptation under natural stimulus conditions. The experiments are done on the H1-cell, an identified neuron in the blowfly visual motion pathway that has served in many previous studies as a model system for visual motion computation. We reconstructed optic flow perceived by a blowfly in free flight and used this behaviorally generated optic flow to study motion adaptation. A variety of measures (variability in spike count, response latency, jitter of spike timing) suggests that the coding quality does not improve with prolonged stimulation. However, although the number of spikes decreases considerably during stimulation with natural optic flow, the amount of information that is conveyed stays nearly constant. Thus the information per spike increases, and motion adaptation leads to parsimonious coding without sacrificing the reliability with which behaviorally relevant information is encoded.

INTRODUCTION

The activity of motion-sensitive neurons in a wide variety of species is known to depend on stimulus history, and the underlying motion-detection mechanisms are often regarded to adapt to prolonged motion stimulation. Motion adaptation has been investigated in motion-sensitive neurons of rabbits (e.g., Barlow and Hill 1963), of wallabies (Ibbotson 1996), of cats (e.g., Azouz and Gray 2003; Giaschi et al. 1993; Marlin 1993, 1991), and of monkeys (e.g., Kohn and Movshon 2003, 2004), but also in insects and, in particular, in blowflies (e.g., Borst and Egelhaaf 1987; de Ruyter van Steveninck et al. 1986; Fairhall et al. 2001; Harris and O'Carroll 2002; Harris et al. 1999, 2000; Kurtz et al. 2000; Maddess and Laughlin 1985; Reisenman et al. 2003; Srinivasan and Dvorak 1979; Zaagman et al. 1983). Despite this great interest in motion adaptation, there is still no coherent view about its functional significance.

In the blowfly, where motion adaptation has been analyzed in particular detail with a wide variety of stimulus paradigms,

several potential advantages and mechanisms of motion adaptation have been discussed. For instance, Maddess and Laughlin (1985) concluded that motion adaptation is a means to enable motion-sensitive neurons to encode velocity changes relative to the actual average velocity (i.e., velocity contrast) irrespective of average velocity. Motion adaptation would thus serve purposes analogous to those of light adaptation in photoreceptors. In other studies, motion adaptation was suggested to maximize the information of spike trains under changing stimulus regimes (Brenner et al. 2000; Fairhall et al. 2001) and to avoid ambiguities in motion coding (Fairhall et al. 2001).

With respect to the mechanisms underlying motion adaptation, it was concluded that prolonged stimulation leads to a reduction of the time constants of the motion-detection mechanism (Borst and Egelhaaf 1987; Borst et al. 2003; Clifford 1997; de Ruyter van Steveninck et al. 1986; Reisenman et al. 2003). The spatially localized character of this reduction suggests that motion adaptation acts presynaptically to the motion-sensitive wide-field neurons that are usually recorded from to analyze motion adaptation (Borst and Egelhaaf 1987; de Ruyter van Steveninck et al. 1986; Maddess and Laughlin 1985). In addition, a postsynaptic mechanism of motion adaptation in blowfly motion-sensitive wide-field neurons was suggested to be the consequence of calcium-dependent potassium channels that shunt the cells during prolonged motion stimulation (Kurtz et al. 2000). Furthermore, after prolonged stimulation an afterhyperpolarization was measured in fly motion-sensitive cells that goes along with a contrast gain reduction (Harris et al. 2000).

All preceding studies on motion adaptation used stimuli that were exclusively designed by the experimenter, such as motion steps (e.g., Borst and Egelhaaf 1987; de Ruyter van Steveninck et al. 1986; Maddess and Laughlin 1985), constant velocity stimuli (e.g., Harris et al. 1999, 2000; Maddess and Laughlin 1985; Reisenman et al. 2003), or white noise velocity fluctuations (Brenner et al. 2000; Fairhall et al. 2001). These stimuli differ substantially with regard to their dynamical properties from the motion stimuli blowflies encounter in free flight. In free flight, the motion flow on the eyes is characterized by peculiar dynamical properties that are the consequence of the characteristic flight and gaze strategy of blowflies: fast saccadic turns with high rotational velocities alternate with flight sections of almost pure translation where gaze is kept virtually stable and the eyes experience mainly translatory optic flow (Schilstra and van Hateren 1998, 1999; van Hateren and

Address for reprint requests and other correspondence: J. Heitwerth, Department of Neurobiology, Faculty for Biology, Bielefeld University, D33501 Bielefeld, Germany (E-mail: jochen.heitwerth@uni-bielefeld.de).

The costs of publication of this article were defrayed in part by the payment of page charges. The article must therefore be hereby marked "advertisement" in accordance with 18 U.S.C. Section 1734 solely to indicate this fact.

Schilstra 1999). In the present study, we use a novel approach that has recently been successfully established (Kern et al. 2005; van Hateren et al. 2005) and use as motion stimuli reconstructions of the natural optic flow perceived by a freely flying fly. We replayed the reconstructed optic flow by a panoramic stimulus device that is appropriate for high-speed presentation of optic flow stimuli (Lindemann et al. 2003) and recorded the spike activity of the H1 neuron of blowflies watching this stimulus. The H1 neuron is one of the motion-sensitive wide-field neurons in the blowfly third visual neuropil (e.g., Hausen and Egelhaaf 1989). We selected this neuron for analysis because it has served as a model system for studying motion adaptation in the blowfly in almost all of the above-mentioned studies. To analyze motion adaptation we used the optic flow as experienced on a closed trajectory and can thus be repeated again and again. In this way we could analyze, for the first time, motion adaptation under a natural stimulus regime. Our findings suggest that prolonged stimulation with natural optic flow leads to parsimonious neuronal coding without sacrificing the reliability of coding performance.

METHODS

Preparation and electrophysiology

Electrophysiological experiments were done on 4- to 7-day-old female blowflies of the genus *Calliphora* that were taken from our laboratory stock. Data of eight H1-cells were analyzed. Dissection was done as described in Dürr and Egelhaaf (1999). The experiments were performed at temperatures between 25 and 30°C that correspond to the head temperature of blowflies during flight (Stavenga et al. 1993). Extracellular recordings were done with electrolytically sharpened tungsten electrodes from the output arborization of the left H1-cell in the right optic lobe. Because H1 is a heterolateral motion-sensitive neuron, it receives its input from the left eye where it is excited by back-to-front motion. Spikes were detected by passing the amplified, band-pass-filtered (LP = 10 kHz; HP = 200 Hz) raw signals through a threshold device that transforms the spikes into uniform pulses. A correct adjustment of the threshold was ensured throughout the experiment. The recordings were sampled at 4 kHz (DT 3001, Data Translation, Marlboro, MA) and stored on hard disk for off-line analysis.

Visual stimulation

The stimulus was based on a free-flight trajectory of *Calliphora vicina*. Both the fly's position in a cubic flight box (edge length, 40 cm) and the head and body orientations were monitored with small sensor coils that were mounted on the fly's head and thorax (Schilstra and van Hateren 1998, 1999; van Hateren and Schilstra 1999). The walls of the flight arena were covered with photographs of herbage. In this setup freely flying flies make about 10 saccadic turns per second. The saccades last for about 20–30 ms and exhibit high rotational velocities. Between saccades, the stabilization of the head orientation reduces the rotational component of the optic flow perceived by the eye, thereby enhancing the relative contribution of the translatory optic flow (Kern et al. 2005).

To analyze the consequences of motion adaptation on coding performance we repeated the same sequence of natural optic flow many times. This procedure allowed us to assess the changes in the response properties of the H1-cell. It required a trajectory with identical start and end position. Because such a perfectly closed trajectory was not available, we generated one from a selected free flight trajectory that had only a small gap between its starting and endpoint. The gap was closed in a naturalistic way by interpolating the

head position and gaze direction according to the following procedure (Fig. 1). We determined the points in space where the yaw velocity of the first and the last saccade of the selected trajectory peaked. These positions were connected linearly in three-dimensional (3-D) space. Because blowflies have basically a straight gaze between saccades, the first and the last saccade had to be modified by appropriately adjusting the yaw, pitch, and roll axis of the head. We set the yaw and roll axes for the interpolated trajectory as if the fly were looking straight into the flight direction. The pitch was set to a value of 11°, according to the mean pitch of the head in natural flight (van Hateren and Schilstra 1999). Gaussian filters were used to smooth out the discontinuities (e.g., yaw in Fig. 1B) between the experimentally determined and the interpolated parts of the trajectory. Figure 1C shows the result for the

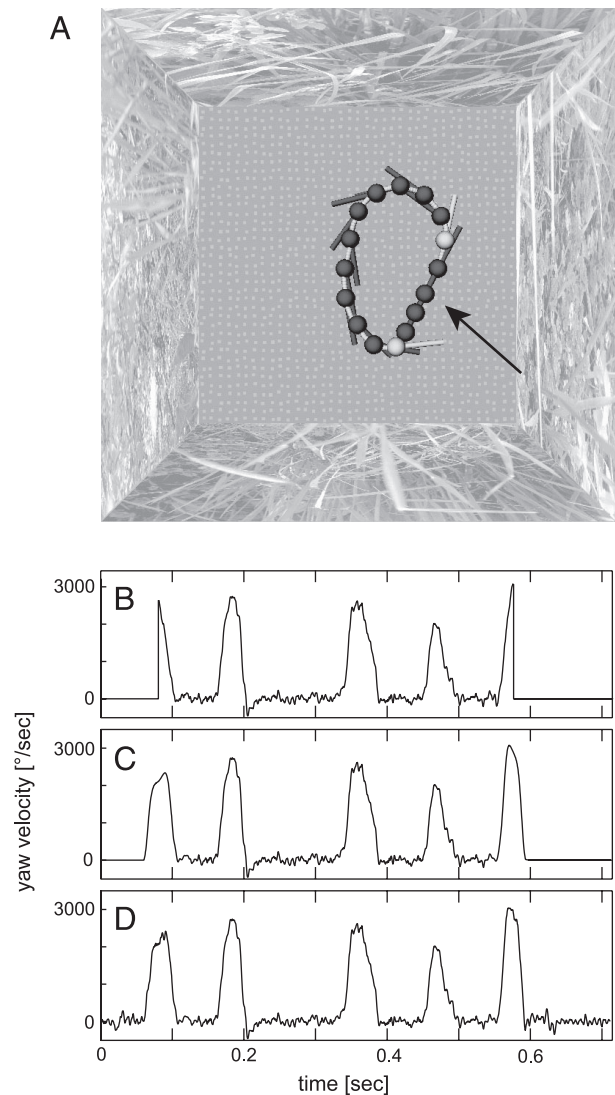


FIG. 1. Natural optic flow stimulus. A: from a natural flight trajectory a segment was selected and closed. Closed flight trajectory is shown in a cubic box with an edge length of 40 cm and walls covered with images of herbage. Position of the head and its orientation are shown every 45 ms by the gray symbols. Light gray symbols mark the first and the last saccade of the closed flight trajectory. Arrow denotes the starting point of the closed flight trajectory. B–D: consequences for yaw velocity of the procedure of closing the selected trajectory (compare METHODS). B: yaw velocity after interpolating along a straight line (see METHODS) between the starting and endpoint of the closed segment of the natural flight trajectory. C: transitions from natural to interpolated trajectory are smoothed. D: natural fluctuations of the yaw velocity were added to the interpolated part of the trajectory. An equivalent procedure was applied to the angular velocities for roll and pitch.

yaw. Finally, the fluctuations in the position and orientation coordinates in free flight were determined and added to the interpolated flight section (Fig. 1D).

With the knowledge of the head position and the gaze direction at any instant of time as well as of the wall texture of the flight arena, we reconstructed the optic flow the animal experienced during flight (for details, see Lindemann et al. 2003). The optic flow reconstructed from the selected trajectory (in the following termed “loop”) can be repeated without any unnatural discontinuities. To analyze motion adaptation we concatenated 15 loops. The resulting stimulus (termed “loop sequence”) lasts for 10.3 s. Loop sequences were repeated between 20 and 150 times for each H1-cell recorded from. Before starting each loop sequence, we faded over 500 ms from a homogeneous field at the mean luminance of the loops to the first frame of the loop sequence. In this way abrupt brightness changes are avoided that may lead to pronounced responses. Between two loop sequences, all light-emitting diodes (LEDs) were set to the mean luminance for 20 s to allow the visual system to return to its preadaptation state. From control experiments we established that a 20-s period is sufficient for this purpose.

The stimuli were presented by FliMax (Lindemann et al. 2003), a device for panoramic and high-speed presentation of behaviorally generated optic flow. FliMax is constructed from 14 of 20 triangular areas of an icosahedron. Over 500 LEDs are attached to each of the 14 triangular areas, so that FliMax consists of over 7,000 LEDs, producing a wide-field stimulus. Its maximum brightness, averaged over the array of LEDs, was 420 cd/m². Movies are shown at a frame rate of 370 frames/s and a spatial resolution of 1.5 to 2.3°. Maximal rotations in our stimulus are about 3,000°/s leading to maximal image jumps between two consecutive frames of about 8° or four to five photoreceptors. However, spatiotemporal aliasing was prevented by spatially and temporally prefiltering the stimulus (for more details see Lindemann et al. 2003; van Hateren et al. 2005).

Data analysis

Data analysis was done with MATLAB Release 13 (The MathWorks, Natick, MA). We analyzed the time courses of neuronal activity, the variability of the neuronal responses, and the precision in spike timing. Each loop contains five saccades, each of which produces optic flow that strongly excites the H1-cell. For the analysis, the onset of a saccade is arbitrarily set to a threshold of 740°/s of the head yaw velocity. The exact value of this threshold does not influence the conclusions reported herein because only changes in response parameters (e.g., latency) during adaptation are interpreted, instead of the absolute values. Spike count is defined as the number of spikes during and after a saccade until the subsequent saccade is generated.

Moreover, we analyzed how well the response of an unadapted H1 neuron can be reconstructed linearly from the response of an adapted H1 neuron responding to the same stimulus. We used the coherence as a measure of reconstruction quality. Given two time-dependent signals, the coherence γ^2 provides a frequency-dependent estimate to what extent the signals can be transformed into each other by linear operations. If γ^2 equals “1” for all frequencies, there is a perfect linear relationship between the two signals that is not contaminated by noise. A coherence value of less than “1” is attributed either to noise or to nonlinearities (Bendat and Piersol 2000). In sensory physiology the coherence is commonly used as a measure to relate a stimulus and the resulting response of a system. In our study we apply the coherence differently. We analyze the relationship between the averaged responses (SIRC = stimulus induced response component) of a non-adapted H1-cell (defined here as the response to loop 1) and the spike trains of an adapted H1-cell (defined here as the response to loop 15). Because the responses of the adapted and the nonadapted cell were elicited by the same stimulus, we can assess how well the adapted response can be predicted from the unadapted one by linear filtering. The coherence between the SIRC of a particular loop and the corre-

sponding individual responses of the same loop represents the expected coherence γ_{exp}^2 . The difference between 1 and the expected coherence reflects the noise inherent in the neuronal responses (van Hateren and Snippe 2001). Thus the expected coherence can be used as a benchmark set by the noise of the system. The difference between the expected coherence and the coherence between nonadapted SIRC and adapted individual responses results from a nonlinear change of the system.

The determination of the coherence and the expected coherence follows previously published procedures (e.g., van Hateren and Snippe 2001).

Thereby, we divided the responses into four time segments overlapping by 50%. These time segments were multiplied by a Hanning window (for details, see sect. 11.5 in Bendat and Piersol 2000). To achieve a better estimate of the coherence for a given cell we first rearranged the data: We built a new data array by concatenating the responses to all loops that are in a certain position within the loop sequence of 15 loops (e.g., concatenating all 1st loops of all trials of a given H1-cell). Accordingly, the SIRC (average of all responses to a particular loop) was concatenated several times to obtain an array of the same length. Between these new data arrays the coherence was calculated according to (for details see van Hateren and Snippe 2001)

$$\gamma^2 = \frac{\langle ft(r)ft(SIRC)^* \rangle \langle ft(SIRC)ft(r)^* \rangle}{\langle ft(SIRC)ft(SIRC)^* \rangle \langle ft(r)ft(r)^* \rangle} \quad (1)$$

The brackets $\langle \rangle$ denote ensemble averages over time segments producing the frequency spectra, $ft(r)$, $ft(SIRC)$ (ft = Fourier transform), of the concatenated responses r and of the concatenated average response $SIRC$, respectively. The $*$ denotes the complex conjugate.

Finally, we determined to what extent the information content of the responses changed as a consequence of motion adaptation by applying a measure that calculates the information without assuming a Gaussian distribution of the stimulus and the responses (Brenner et al. 2000; van Hateren et al. 2002)

$$I(1\text{spike}) = \frac{1}{T} \int_0^T \left(\frac{r(t)}{\bar{r}} \right) \log_2 \left(\frac{r(t)}{\bar{r}} \right) \quad (2)$$

where $r(t)$ is the time-dependent spike rate, \bar{r} is the time-average of the spike rate, and T is the length of the response segment. Equation 2 provides the information per spike from the spike-frequency histogram and the mean spike rate of the responses to a stimulus, thus ignoring higher-order structure in the spike train. For the H1 neuron, it gives a reasonably accurate estimate of the information per spike (see Brenner et al. 2000). The information per spike multiplied with the spike rate of each loop yields the information rate of each loop.

RESULTS

To assess whether the visual motion pathway of the blowfly adapts during natural flight behavior, we repeated the optic flow based on a measured flight trajectory (“loop”) 15 times (“loop sequence”). The measured trajectory was almost a complete loop, which was fully closed by tuning the first and last saccades of the original trajectory in accordance with the properties of naturally occurring saccades (Fig. 1 and METHODS). We could not detect any systematic difference in the responses of the spiking H1 neuron to the tuned and the natural saccades (see Figs. 2, 4, and 5). Thus there was no need to exclude the responses to the tuned saccades from the analysis. Previous studies with simple experimenter-defined stimuli showed that motion adaptation takes place on timescales between some hundreds of milliseconds and a few seconds (Borst

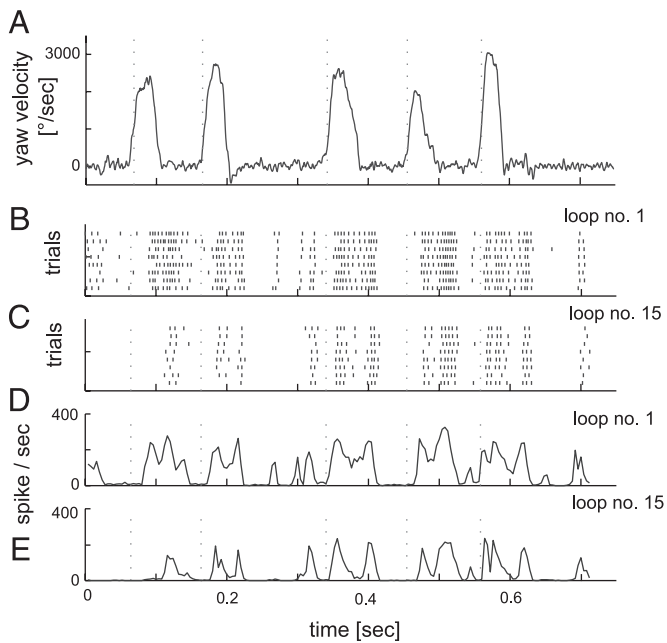


FIG. 2. Responses of the H1 neuron to the natural optic flow stimulus. *A*: yaw velocity as in Fig. 1*D*. *B*: raster of consecutive individual responses of the H1 to the 1st loop in the loop sequence. Time of occurrence of each spike is indicated by a vertical line. *C*: individual H1 responses to the 15th loop in the loop sequence. *D*: spike frequency histogram of the responses to the 1st loop (104 trials). *E*: spike frequency histogram of the responses to the 15th loop (104 trials). *A–E*: Vertical broken lines denote the onset of the saccades (i.e., times when the yaw rotation exceeds 740°/s for the first time after the onset of a saccade).

and Egelhaaf 1987; de Ruyter van Steveninck et al. 1986; Fairhall et al. 2001; Kurtz et al. 2000; Maddess and Laughlin 1985; Srinivasan and Dvorak 1979; Zaagman et al. 1983). Therefore we selected a relatively short loop, lasting for only about 700 ms to minimize motion adaptation already during the first loop of the loop sequence. Loop sequences were repeated, after a 20-s waiting time sufficient to let the system return to its unadapted state.

The H1 neuron is excited best by horizontal back-to-front motion in its receptive field in front of the eye contralateral to the recording electrode, although its direction tuning is broad (Eckert 1980; Hausen 1976). When the H1 neuron obtaining input from the left visual hemisphere is stimulated with behaviorally generated optic flow it is thus excited during leftward saccades. Because our stimulus sequence originated from a flight trajectory segment constituting leftward saccades only, the left-eye H1-cell was strongly activated during each saccade (Fig. 2, *B–E*). H1 responds with a burst of spikes shortly after the onset of a saccade. Between bursts resulting from consecutive saccades H1 is inhibited by the translatory optic flow dominating between saccades because of gaze stabilization (see van Hateren and Schilstra 1999). Nonetheless, spikes are generated sometimes even between saccades. These responses are probably the consequence of back-to-front motion components in the complex natural optic flow that may be related to sideward drift of the animal (Kern et al. 2005; van Hateren et al. 2005).

As can be seen in Fig. 2, the response to the last loop of the loop sequence shows fewer spikes than the response to the first loop, although the overall pattern of spike activity is similar (compare Fig. 2*B* and 2*C*). Spike frequency histograms deter-

mined by averaging over all repetitions of the loop sequence for a given cell (Fig. 2, *D* and *E*) corroborate this view. During the first loop the peak activity assumes spike rates between 210 spikes/s and occasionally even more than 300 spikes/s depending on the saccade. In the 15th loop the activity peaks are considerably smaller, ranging between 150 and 230 spikes/s.

The changes in activity and more subtle changes in the response properties of H1 that go along with the repeated presentation of the same loop are quantified in the subsequent sections.

Spike count and spike count variability

The average number of spikes per saccade (“spike count”; see METHODS) of a loop decreases by about 45% during maintained stimulation with behaviorally generated optic flow (Fig. 3*A*). The spike count also consistently decreases as a function of loop number for each of the five saccades (data not shown). The magnitude of the decrement appears to be independent of the overall response amplitude evoked by a given saccade. The decrease levels off after presentation of four to five loops, roughly corresponding to 3–4 s of stimulation.

The spike count variance across trials also slightly decreases, although the large SDs make it hard to draw firm conclusions (Fig. 3*B*). Accordingly, the Fano factor (i.e., the ratio between spike count variance and mean spike count) stays almost constant during the loop sequence, seemingly with a slight tendency to increase. As shown in Fig. 3*C* all values of the Fano factor determined in this study range from 0.3 to 0.5. These values are much lower than expected from a Poisson process of spike generation and as observed in the visual cortex of cats and monkeys (Barberini et al. 2001; Tolhurst et al. 1983; Vogels et al. 1989), but are in accordance with earlier

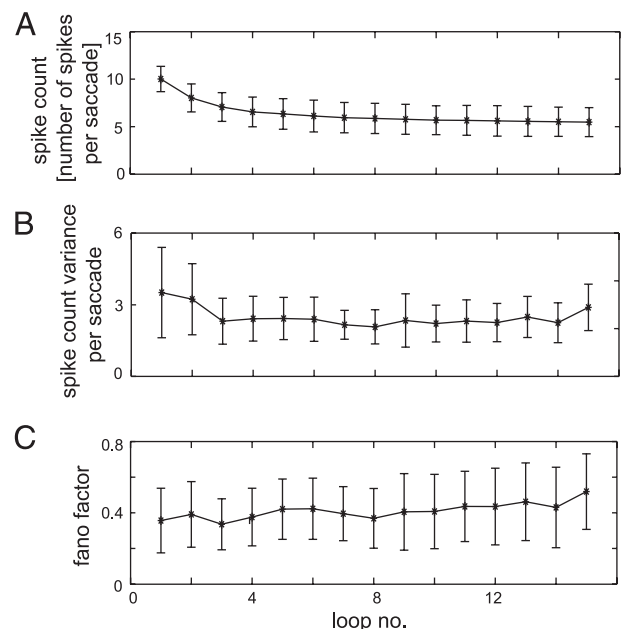


FIG. 3. Mean spike count (*A*), spike count variance (*B*), and Fano factor (*C*) (i.e., the variance divided by the mean) as a function of the loop number as averaged over saccades and flies (8 flies with 20 to 150 trials per fly). Bars denote the SD over the flies. Mean spike count and the variance of the spike count decrease with increasing loop number. As a consequence, the Fano factor increases only slightly with increasing loop number.

measurements on H1 with conventional experimenter-designed stimuli (de Ruyter van Steveninck et al. 1997; Warzecha and Egelhaaf 1999; Warzecha et al. 2000). In any case, the responses of H1 do not become more reliable, as quantified by the Fano factor, during prolonged stimulation with behaviorally generated optic flow.

Precision of spike timing

The left-eye H1-cell responds with a burst of spikes to leftward saccades. The timing of the first spike of a burst may be crucial for the information conveyed by the neuron (Panzeri et al. 2001). Thus we scrutinized the timing of the first spike and analyzed the latency and the jitter of the first spike of the bursts. We define the latency as the interval from the beginning of a saccade to the occurrence of the first spike of the corresponding burst. Note that because the threshold criterion for the onset of a saccade (see METHODS) is somewhat arbitrary, it is not surprising that the latencies determined in this way differ substantially for different saccades (Fig. 4A, different symbols). This variability is not critical for the analysis because we are interested in latency *changes* as a consequence of repetitive presentation of the same loop rather than in absolute latency values. For all saccades the latency of the first spike within a burst increases, although to a different extent, ranging between 3 and 10 ms (averaged over eight H1 neurons; Fig. 4, A and B). The increment levels off after four to five repetitions of the loop.

The jitter in spike timing is defined here as the SD of the timing of the first spike in each individual burst relative to a fixed reference point. The values for the jitter scatter around 3

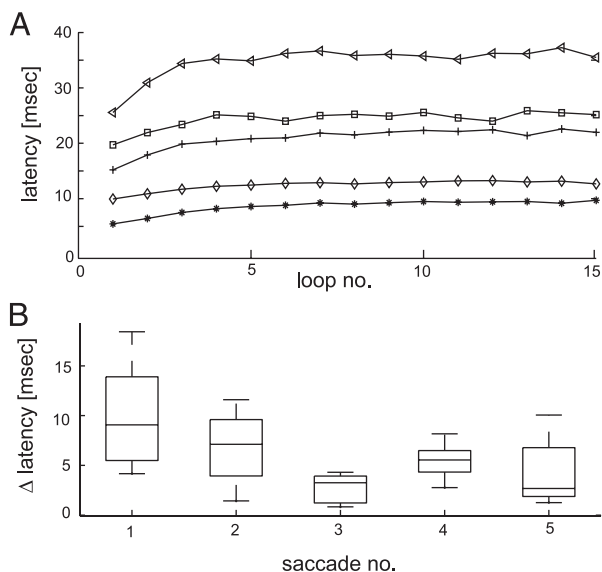


FIG. 4. Latency changes as a consequence of motion adaptation. A: mean latency of the first spike within the spike burst in response to each of the 5 saccades as a function of the number of the loop in the loop sequence. Triangles, crosses, diamonds, squares, and asterisks denote the latencies for *saccade 1* to *saccade 5*, respectively. Mean latency is calculated as the average over the trials and the average over 8 H1-cells. Wide range of latencies is a consequence of the definition of saccade onset (see METHODS and Fig. 2A). B: change of mean latency of the first spike after saccades between loop 1 and loop 15. For all 5 saccades the mean latency increases. Midlines of the boxes denote the medians, the *top* and *bottom* lines the quartiles, and the whiskers show the extent of the rest of the data ($n = 8$ flies).

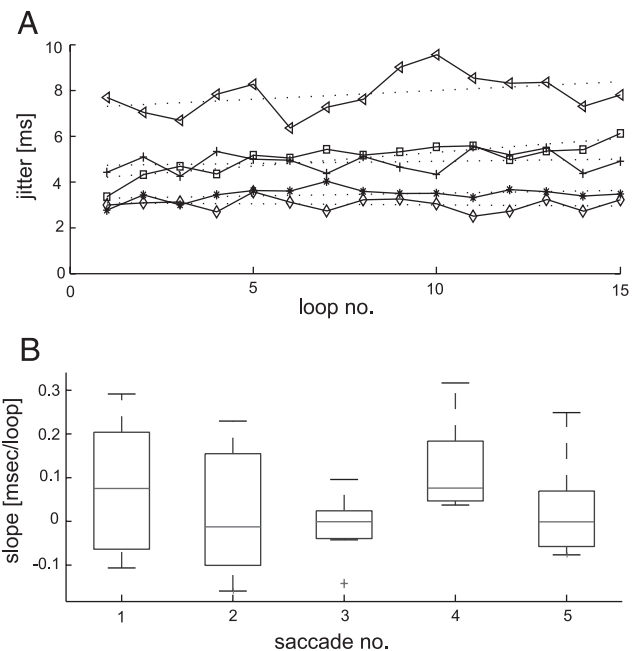


FIG. 5. Temporal precision ("jitter") of the first spike evoked by a saccade. A: mean jitter obtained from 8 H1-cells of the first spike evoked by each of the 5 saccades (different symbols) is plotted as a function of the loop number within the loop sequence. Jitter is calculated as the SD of the latency of the first spike evoked by a saccade. Dotted lines represent the results of linear regression analysis. Triangles, crosses, diamonds, squares, and asterisks denote *saccade 1* to *saccade 5*, respectively. B: for each saccade and each of 8 H1-cells a regression line is determined of the dependency of the jitter of the first spike on the loop number within the loop sequence. A box plot of the slopes of the regression lines is shown for each of the saccades. Midlines of the boxes denote the medians, the *top* and *bottom* lines the quartiles, and the whiskers show the extent of the rest of the data ($n = 8$ flies) except for the outlier for *saccade 3* (indicated by the +). There is no consistent change with motion adaptation of the jitter for the 5 saccades.

ms for the response burst with the highest timing precision (*saccade 3*, diamonds) and around 8 ms for the response burst with the lowest timing precision (*saccade 1*, triangles) (Fig. 5A). For each of the five saccades the jitter varies over the 15 loops, although it is hard to see a consistent trend. To assess whether there is a trend, we determined a linear regression for each saccade and each neuron. The resultant slopes of the regressions of the eight H1-cells have medians of 0.075, -0.01, 0, 0.075, and 0, for *saccades 1* to *5*, respectively (given in milliseconds per loop; temporal resolution of spike time 0, 25 ms; Fig. 5B). Thus if there is a trend at all, it is a slight increment in the jitter. However, considering the small slopes and the variability of the jitter (as indicated by the large quartiles and margins/whiskers in Fig. 5B) it appears that adaptation does not unambiguously affect the timing precision of the first spikes of response bursts evoked by saccades.

Changes in the overall time course of the responses

Although the timing of the first spike of a saccade-evoked burst may be of particular functional significance, this measure does not account for potential changes of the timing of spikes within a burst. A potential change in the time course of the neuronal responses across loops was therefore assessed by determining their similarity based on a coherence analysis. In other words, we assessed how well the stimulus-induced re-

sponse component (SIRC) for the first presentation of the loop as given by the spike frequency histogram can be predicted from individual responses evoked by the 15th presentation. The similarity between the experimentally determined SIRC and the predicted one is quantified by the coherence (see METHODS). The coherence is a frequency-dependent measure that varies between 0 (i.e., both signals are unrelated) and 1 (i.e., perfect reconstruction). The expected coherence represents a benchmark of the upper limit of the coherence that can be expected, if the responses are affected only by noise and not by some sort of nonlinear transformation (see METHODS).

The coherence between the individual responses to loop 15 and the SIRC of loop 1 has a maximum of >0.7 at low frequencies (Fig. 6, triangles). The coherence decreases slightly with increasing frequency, but stays >0.6 up to 25 Hz. Only then does it drop steeply and reach almost 0 at about 100 Hz (Fig. 6). The expected coherence for loop 1 (Fig. 6, plus signs) and the expected coherence for loop 15 (Fig. 6, diamonds) are about 0.85 at low frequencies and stay >0.7 up to about 25 Hz. Then the expected coherences decrease steeply and reach a level of almost 0 at about 100 Hz. The coherence between the individual responses to loop 15 and the SIRC of loop 1 is smaller by only about 0.15 than the expected coherences at all frequencies between 3 and 30 Hz. This feature indicates that changes in the neuronal responses to prolonged stimulation with behaviorally generated optic flow can, to a large extent, be accounted for by a linear transformation, as is already suggested by the similar shape of the spike frequency histograms for loop 1 and loop 15 (compare Fig. 2, *D* and *E*). Nonetheless, the differences between the coherence and the expected coherences suggest that a nonlinearity somewhere in the motion pathway plays a significant role in shaping the response changes during prolonged motion stimulation.

Information conveyed by spikes

As shown earlier (Fig. 3*A*), the number of spikes evoked by behaviorally generated optic flow decreases by about 45% after

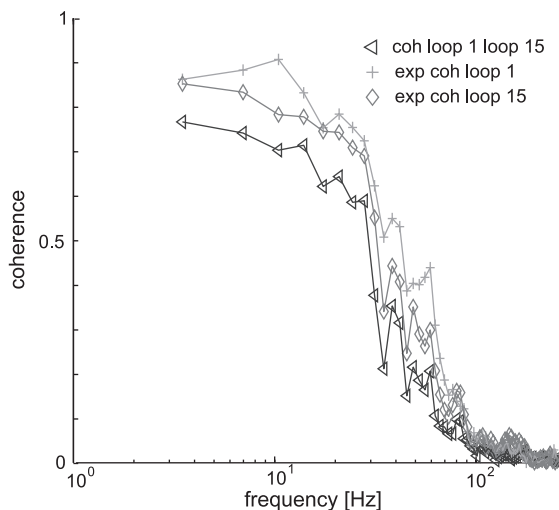


FIG. 6. Coherence between the signal-induced response component (SIRC) of the 1st loop and the spike trains of the 15th loop (triangles) and the expected coherences of the 1st (plus signs) as well as the 15th loop (diamonds). Difference between 1 and the expected coherence is explained by the noise of the system. Difference between coherence and expected coherence arises from nonlinear changes of the system.

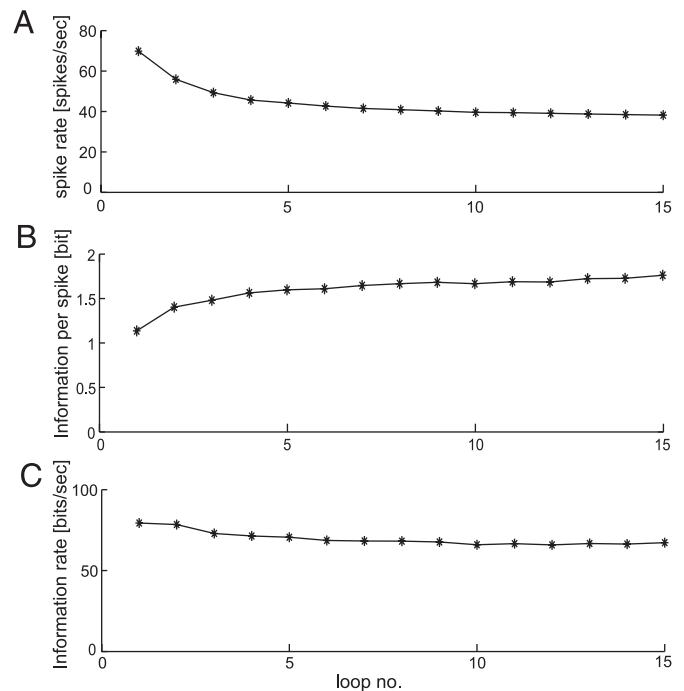


FIG. 7. Information conveyed by neuronal responses before and after motion adaptation. *A*: mean spike rate as a function of the loop number. *B*: average information transmitted by single spikes as a function of the loop number. *C*: information rate transmitted by the response to a loop as a function of the loop number. Because the mean spike rate decreases and the information per spike increases, the information rate is nearly independent of the loop number.

repeated presentation of the same loop. Because in previous studies the information conveyed by responses of the H1 neuron to experimenter-defined stimuli was found to decrease substantially with decreasing spike count (Borst and Haag 2001; Schneidman et al. 2001), we analyzed whether the transmitted information during stimulation with behaviorally generated optic flow is reduced in a similar way.

As is clear from Fig. 7*B*, the information transmitted per spike (see METHODS) increases with prolonged stimulation (increment of 55%; Fig. 7*B* was calculated with a temporal resolution of 1 ms; similar results were obtained with 0.5, 2, and 4 ms). Thus the information rate in each loop (see METHODS) decreases much less (from 79 bits/s in loop 1 to 67 bits/s in loop 15, a reduction of 15%; Fig. 7*C*) than the spike rate (reduction of 45%; Fig. 7*A*). Thus only a slightly smaller amount of information is conveyed by a considerably smaller number of spikes (compare Fig. 7*C* and 7*A*). Thus information transfer appears to be more parsimonious in H1 after motion adaptation.

DISCUSSION

Motion adaptation is often regarded not only as a change in the response properties of motion-sensitive neurons, but also as an improvement of system performance (Borst and Egelhaaf 1987; de Ruyter van Steveninck et al. 1986; Fairhall et al. 2001; Harris et al. 2000; Maddess and Laughlin 1985). Here we show, in the first study of motion adaptation using behaviorally generated optic flow, that after motion adaptation nearly the same amount of information is transmitted as before motion adaptation. However, this information is transmitted by con-

siderably fewer spikes. Accordingly, the spike count variability, the timing precision, the response latency, and the information rate did not change as a consequence of prolonged stimulation. Thus under natural behaviorally generated stimulus conditions motion adaptation ensures parsimonious neuronal coding without affecting coding performance.

The strength of motion adaptation shown here probably represents an upper bound of the adaptation occurring in natural circumstances. Because we had to present the same relatively short natural motion sequence repetitively for analyzing motion adaptation the selected closed flight trajectory had to be short. Consequently, the saccades in each loop are large and exclusively into the preferred direction of the analyzed H1 neuron. Although flights containing an extended series of large saccades into one direction occasionally occur (van Hateren, unpublished observations), the more common situation is a mixture of small and large saccades, frequently changing between leftward and rightward (van Hateren and Schilstra 1999). For such stimuli, the adaptation is expected not to be as strong as reported here because a particular H1 neuron will be less strongly stimulated. This prediction is corroborated by a recent study modeling the responses of a wide-field motion-sensitive neuron of the fly to optic flow as experienced in diverse flights (Lindemann et al. 2005). The statistics of these flights were not as extreme as the loop that had to be used in the present study. In the study cited it was concluded that there is some reduction in the overall gain of the system (about 26%) without any obvious consistent changes in other systems parameters (such as time constants).

Natural motion stimuli as a means to analyze motion computation

In recent studies, natural motion stimuli were approximated in various ways. Using natural images moving at constant velocities the velocity tuning could be shown to be much more robust to texture changes than stimuli consisting of only a few spatial frequency components (Dror et al. 2001). Moreover, Lewen et al. (2001) rotated blowflies in a natural setting with an angular velocity that was related to the angular velocity of a flight trajectory of another fly. In neither case, did the dynamics of the motion stimuli correspond to the dynamics as is characteristic of the peculiar saccadic flight and gaze strategy of blowflies (Schilstra and van Hateren 1999; van Hateren and Schilstra 1999). Natural gaze dynamics has been shown to be essential, if correct conclusions about the coding properties of blowfly motion-sensitive neurons are to be drawn (Kern et al. 2005; van Hateren et al. 2005). Therefore we analyzed motion adaptation by stimulating the fly with exactly the motion dynamics occurring in free flight *including* the rotations around all body axes. Although we used natural images on the walls of our flight arena, this stimulus feature is likely to be of only minor relevance compared with stimulus dynamics: the responses to behaviorally relevant optic flow are relatively robust to changes in pattern texture (Lindemann et al. 2005).

Comparison with other studies on motion adaptation

Prolonged motion stimulation has been shown previously—in accordance with our results—to reduce response amplitudes (Fairhall et al. 2001; Harris et al. 2000; Kurtz et al. 2000;

Maddess and Laughlin 1985; Reisenman et al. 2003). This reduction in response amplitude was concluded to be the consequence of a decrease in the motion contrast gain of the system, but also of a subtractive shift of the relationship between stimulus strength and response amplitude (Harris et al. 2000). Given the rectification nonlinearity of the spiking H1 neuron analyzed in the present study, this shift could be one reason for the weak nonlinearity that characterizes the relationship between the unadapted and the adapted responses (Fig. 6). Such a subtractive shift could sharpen the time course of the response to behaviorally generated optic flow and eventually result in a higher information content per spike (Eq. 2).

The observed gain reduction could have its origin presynaptically to the H1-cell or in the H1-cell itself. A postsynaptic gain reduction is suggested for blowfly HS and CH cells (tangential cells like the H1-cell) on the basis of experiments measuring the intracellular Ca^{2+} accumulation during prolonged motion stimulation into the preferred direction (Kurtz et al. 2000). The Ca^{2+} accumulation could lead to the opening of Ca^{2+} -dependent K^{+} channels resulting in a hyperpolarization of the tangential cell and a reduction of its input resistance. A similar Ca^{2+} -dependent gain control mechanism, however, is also conceivable at the level of local elements presynaptic to the tangential cell. Irrespective of the mechanism underlying gain reduction in the visual motion pathway, fewer spikes in the saccade-triggered burst responses may well lead to the observed small increase in latency of the first spike. Thus the previous results on gain reduction as a consequence of prolonged motion stimulation are consistent with the findings of the present study.

Earlier studies concluded that prolonged stimulation leads to a reduction of the time constant of the local motion detection mechanism, suggesting that motion adaptation acts presynaptic to motion-sensitive tangential cells such as the H1-cell (Borst and Egelhaaf 1987; Borst et al. 2003; Clifford 1997; de Ruyter van Steveninck et al. 1986; Maddess and Laughlin 1985; Reisenman et al. 2003). It may well be possible that the adaptational changes reported here are attributed not only to a gain reduction but also to changes in the time constants in the visual motion pathway. However, other studies concluded that motion adaptation might not require parameter changes of the local motion detectors (Borst et al. 2005; Harris et al. 1999).

Because one loop of our behaviorally generated motion stimuli lasted for somewhat >700 ms, we cannot exclude adaptational changes at shorter timescales, such as were concluded to exist on the basis of experiments using white noise velocity fluctuations with an almost flat spectrum ≤ 250 Hz (Fairhall et al. 2001). Because the fast adaptational mechanisms proposed by Fairhall et al. (2001) rely on the detection of changes in stimulus statistics, especially in the high-frequency range, these mechanisms are likely to be of only minor importance for the natural operating conditions of the H1 neuron. The dynamics of natural optic flow is mainly shaped by sequences of saccades and intersaccadic intervals that may occur at a rate of ≤ 10 Hz (Schilstra and van Hateren 1999; van Hateren and Schilstra 1999). Moreover, blowfly motion-sensitive neurons, such as the H1-cell, contain information about self-motion of the animal and the 3-D layout of the environment mainly in a frequency range < 40 Hz (Kern et al. 2005; van Hateren et al. 2005), which is the same frequency band in which the input has its highest power (Kern et al. 2005).

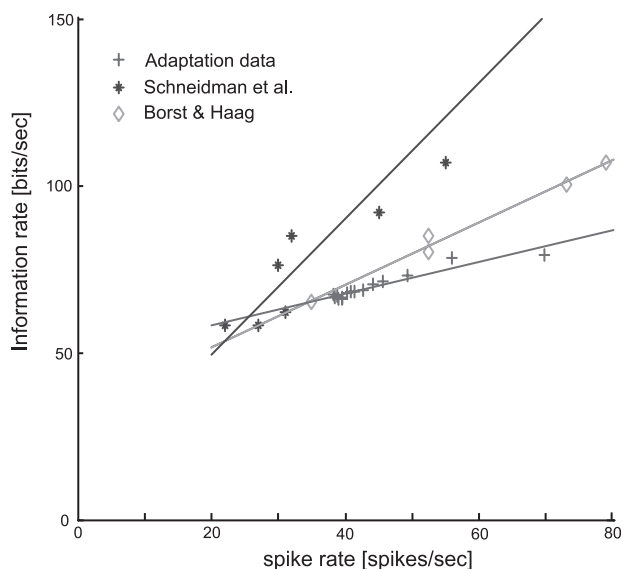


FIG. 8. Comparison between studies. Information rate is plotted as a function of the mean activity. Data are derived from Schneidman et al. (2001; asterisks) and from Borst and Haag (2001; diamonds). Crosses are derived from Fig. 7. Slopes for the regression lines of the adaptation data are much lower (0.48Δ bits per Δ spike) than the slopes of the regression lines for the data of Schneidman et al. (2001; 2.04Δ bits per Δ spike) and Borst and Haag (2001; 0.93Δ bits per Δ spike).

Functional consequences of motion adaptation

The small increment of the latency of the first spike after the start of a saccade is in the range of its temporal jitter. Thus on the basis of single spike trains it is difficult to distinguish by means of the latency whether the cell is in an adapted or in a nonadapted state. This finding suggests that the latency increment is not a critical aspect for the coding of the H1-cell.

Although the spike rate decreases with prolonged stimulation with behaviorally generated optic flow, the information rate of each loop decreases only slightly. From the data obtained with exclusively experimenter-defined motion stimuli published in previous studies (Borst and Haag 2001; Schneidman et al. 2001), a much stronger decrease in total information with decreasing spike rate would have been expected (Fig. 8). In contrast to our study, Schneidman et al. (2001) and Borst and Haag (2001) did not alter the spike rate by motion adaptation, but by changing various stimulus parameters. Thus it appears that the surprisingly small decline in information rate found in our experiments is not the consequence of the declined spike rate per se but a consequence of motion adaptation. This conclusion is corroborated by the fact that if only the spike rate would be scaled down by a given factor during motion adaptation, the information rate should decrease by exactly the same factor because the information per spike stays constant (see Eq. 2). The increase in the information transmitted by single spikes must therefore be the consequence of other changes occurring during motion adaptation, such as the above-mentioned nonlinearity resulting possibly from a subtractive shift in the responses during motion adaptation (Harris et al. 2000) combined with the rectification properties of the H1 neuron (compare also Fig. 2, C and D).

We have shown that for behaviorally generated optic flow nearly the same amount of information that is transmitted in the adapted state is mediated by 55% of the initial spike rate. Thus

motion adaptation leads to parsimonious coding without sacrificing coding accuracy. This feature might be adaptive because spikes are very costly from an energetic perspective (see, e.g., Attwell and Laughlin 2001). It has been estimated for gray matter of the rodent brain that even at very low average firing rates of only 4 Hz almost 50% of the energy expenditure of nerve cells related to neuronal signaling arises from spike generation (Attwell and Laughlin 2001). This percentage is likely to be much higher for neurons with spike rates as high as that of the H1-cell. Thus much energy could be saved during prolonged stimulation with behaviorally generated optic flow when coding becomes more parsimonious, in particular in flight segments with large saccades. Although this conclusion is suggestive from a functional perspective, conclusions concerning energy efficiency have to be drawn cautiously, as long as it is not known how expensive spikes are in the unadapted and the adapted states. For example, if an adaptation mechanism would be mediated by a shunting inhibition in the H1 neuron (Kurtz et al. 2000) the membrane resistance would be reduced and thereby more ionic influx would be needed to depolarize the membrane such that it could reach the firing threshold. For each spike this would result in a higher energy expenditure. Moreover, some components of adaptation presumably occur in the local elements feeding into the H1-cell (Borst and Egelhaaf 1987; Borst et al. 2003, 2005; Clifford 1997; de Ruyter van Steveninck et al. 1986; Reisenman et al. 2003) of which few physiological details are known. Therefore knowledge of the energetical constraints imposed on the neuronal signaling in this system is still rather limited.

The H1-cell shows its strongest responses during saccades and is largely inhibited during translational movements between saccades. A previous study (van Hateren et al. 2005) therefore concluded that the H1-cell may play an important role in preventing, by an inhibitory cell, saccadic responses of a neuron involved in object detection. Although the responses to saccades become smaller during motion adaptation, saccades are still detected with similar accuracy. Thus saccadic suppression may not deteriorate as a consequence of motion adaptation. This hypothesis will be one topic in further experimental studies.

In conclusion, we analyzed for the first time motion adaptation under natural stimulus conditions. Even though the number of spikes decreases much during adaptation, the amount of information that is conveyed stays nearly constant. Moreover, the coding quality does not appear to deteriorate despite the decrease in the overall number of spikes. Thus motion adaptation leads to parsimonious coding of behaviorally generated optic flow without sacrificing coding quality. Because spikes are very costly from an energetic perspective (see, e.g., Attwell and Laughlin 2001), it is conceivable that the most significant effect of motion adaptation under natural behavioral conditions could be to reduce the energetic costs during flight maneuvers lasting for more than a couple of seconds.

ACKNOWLEDGMENTS

The authors are grateful to R. Kurtz for critically reading the manuscript.

GRANTS

This work was supported by Deutsche Forschungsgemeinschaft.

REFERENCES

- Attwell D and Laughlin SB.** An energy budget for signaling in the grey matter of the brain. *J Cereb Blood Flow Metab* 21: 1133–1145, 2001.
- Azouz R and Gray CM.** Adaptive coincidence detection and dynamic gain control in visual cortical neurons in vivo. *Neuron* 37: 513–523, 2003.
- Barberini CL, Horwitz GD, and Newsome WT.** A comparison of spiking statistics in motion sensing neurones of flies and monkeys. In: *Motion Vision—Computational, Neural, and Ecological Constraints*, edited by Zanker JM and Zeil J. New York: Springer Verlag, 2001.
- Barlow HB and Hill RM.** Selective sensitivity to direction of movement in ganglion cells of the rabbit retina. *Science* 139: 412–414, 1963.
- Bendat JS and Piersol AG.** *Random Data: Analysis and Measurement Procedures*. New York: Wiley-Interscience, 2000.
- Borst A and Egelhaaf M.** Temporal modulation of luminance adapts time constant of fly movement detector. *Biol Cybern* 56: 209–215, 1987.
- Borst A, Flanagan VL, and Sompolinsky H.** Adaptation without parameter change: dynamic gain control in motion detection. *Proc Natl Acad Sci USA* 102: 6172–6176, 2005.
- Borst A and Haag J.** Effects of mean firing on neural information rate. *J Comput Neurosci* 10: 213–221, 2001.
- Borst A, Reisenman C, and Haag J.** Adaptation of response transients in fly motion vision. II: Model studies. *Vision Res* 43: 1311–1324, 2003.
- Brenner N, Strong SP, Koberle R, Bialek W, and de Ruyter van Steveninck R.** Synergy in a neural code. *Neural Comput* 12: 1531–1552, 2000.
- Clifford CW, Ibbotson MR, and Langley K.** An adaptive Reichardt detector model of motion adaptation in insects and mammals. *Vis Neurosci* 14: 741–749, 1997.
- de Ruyter van Steveninck RR, Lewen GD, Strong SP, Koberle R, and Bialek W.** Reproducibility and variability in neural spike trains. *Science* 275: 1805–1808, 1997.
- de Ruyter van Steveninck RR, Zaagman WH, and Mastebroek HAK.** Adaptation of transient responses of a movement-sensitive neuron in the visual system of the blowfly *Calliphora erythrocephala*. *Biol Cybern* 54: 223–236, 1986.
- Dror RO, O'Carroll DC, and Laughlin SB.** Accuracy of velocity estimation by Reichardt correlators. *J Opt Soc Am A Opt Image Sci Vis* 18: 241–252, 2001.
- Dürr V and Egelhaaf M.** In vivo calcium accumulation in presynaptic and postsynaptic dendrites of visual interneurons. *J Neurophysiol* 82: 3327–3338, 1999.
- Eckert H.** Functional properties of the H1 neuron in the third optical ganglion of the blowfly, *Phaenecia*. *J Comp Physiol A Sens Neural Behav Physiol* 29–39, 1980.
- Fairhall AL, Lewen GD, Bialek W, and de Ruyter van Steveninck RR.** Efficiency and ambiguity in an adaptive neural code. *Nature* 412: 787–792, 2001.
- Giaschi D, Douglas R, Marlin S, and Cynader M.** The time course of direction-selective adaptation in simple and complex cells in cat striate cortex. *J Neurophysiol* 70: 2024–2034, 1993.
- Harris RA and O'Carroll DC.** Afterimages in fly motion vision. *Vision Res* 42: 1701–1714, 2002.
- Harris RA, O'Carroll DC, and Laughlin SB.** Adaptation and the temporal delay filter of fly motion detectors. *Vision Res* 39: 2603–2613, 1999.
- Harris RA, O'Carroll DC, and Laughlin SB.** Contrast gain reduction in fly motion adaptation. *Neuron* 28: 595–606, 2000.
- Hausen K.** *Struktur, Funktion und Konnektivität bewegungsempfindlicher Interneurone im dritten optischen Nueropil der Schmeißfliege Calliphora erythrocephala* (Dissertation). Tübingen, Germany: Universität Tübingen, 1976.
- Hausen K and Egelhaaf M.** Neural mechanisms of visual course control in insects. In: *Facets of Vision*, edited by Stavenga D and Hardie RC. New York: Springer-Verlag, 1989, p. 391–424.
- Ibbotson MR and Mark RF.** Impulse responses distinguish two classes of directional motion-sensitive neurons in the nucleus of the optic tract. *J Neurophysiol* 75: 996–1007, 1996.
- Kern R, van Hateren JH, Michaelis C, Lindemann JP, and Egelhaaf M.** Function of a fly motion-sensitive neuron matches eye movements during free flight. *PLoS Biol* 3: e171, 2005.
- Kohn A and Movshon JA.** Neuronal adaptation to visual motion in area MT of the macaque. *Neuron* 39: 681–691, 2003.
- Kohn A and Movshon JA.** Adaptation changes the direction tuning of macaque MT neurons. *Nat Neurosci* 7: 764–772, 2004.
- Kurtz R, Dürr V, and Egelhaaf M.** Dendritic calcium accumulation associated with direction selective adaptation in visual motion sensitive neurons in vivo. *J Neurophysiol* 84: 1914–1923, 2000.
- Lewen GD, Bialek W, and de Ruyter van Steveninck RR.** Neural coding of naturalistic motion stimuli. *Network* 12: 317–329, 2001.
- Lindemann JP, Kern R, Michaelis C, Meyer P, van Hateren JH, and Egelhaaf M.** FliMax, a novel stimulus device for panoramic and highspeed presentation of behaviourally generated optic flow. *Vision Res* 43: 779–791, 2003.
- Lindemann JP, Kern R, van Hateren JH, Ritter H, and Egelhaaf M.** On the computations analysing natural optic flow: quantitative model analysis of the blowfly motion vision pathway. *J Neurosci* In press.
- Maddess T and Laughlin SB.** Adaptation of the motion-sensitive neuron H1 is generated locally and governed by contrast frequency. *Proc R Soc Lond B Biol Sci* 225: 251–275, 1985.
- Marlin S, Douglas R, and Cynader M.** Position-specific adaptation in complex cell receptive fields of the cat striate cortex. *J Neurophysiol* 69: 2209–2221, 1993.
- Marlin SG, Douglas RM, and Cynader MS.** Position-specific adaptation in simple cell receptive fields of the cat striate cortex. *J Neurophysiol* 66: 1769–1784, 1991.
- Panzeri S, Petersen RS, Schultz SR, Lebedev M, and Diamond ME.** The role of spike timing in the coding of stimulus location in rat somatosensory cortex. *Neuron* 29: 769–777, 2001.
- Reisenman C, Haag J, and Borst A.** Adaptation of response transients in fly motion vision. I: Experiments. *Vision Res* 43: 1291–1307, 2003.
- Schilstra C and van Hateren JH.** Stabilizing gaze in flying blowflies. *Nature* 395: 654, 1998.
- Schilstra C and van Hateren JH.** Blowfly flight and optic flow. I. Thorax kinematics and flight dynamics. *J Exp Biol* 202: 1481–1490, 1999.
- Schneidman E, Brenner N, Tishby N, de Ruyter van Steveninck R, and Bialek W.** Universality and individuality in a neural code. In: *Advances in Neural Information Processing*, edited by Leem TKD. Cambridge, MA: MIT Press, 2001, vol. 13, p. 151–165.
- Srinivasan MV and Dvorak DR.** The waterfall illusion in an insect visual system. *Vision Res* 19: 1435–1437, 1979.
- Stavenga DG, Schwering PBW, and Tinbergen J.** A three-compartment model describing temperature changes in tethered flying blowflies. *J Exp Biol* 185: 326–333, 1993.
- Tolhurst DJ, Movshon JA, and Dean AF.** The statistical reliability of signals in single neurons in cat and monkey visual cortex. *Vision Res* 23: 775–785, 1983.
- van Hateren JH, Kern R, Schwerdtfeger G, and Egelhaaf M.** Function and coding in the blowfly H1 neuron during naturalistic optic flow. *J Neurosci* 25: 4343–4352, 2005.
- van Hateren JH, Rüttiger L, Sun H, and Lee BB.** Processing of natural temporal stimuli by macaque retinal ganglion cells. *J Neurosci* 22: 9945–9960, 2002.
- van Hateren JH and Schilstra C.** Blowfly flight and optic flow. II. Head movements during flight. *J Exp Biol* 202: 1491–1500, 1999.
- van Hateren JH and Snippe HP.** Information theoretical evaluation of parametric models of gain control in blowfly photoreceptor cells. *Vision Res* 41: 1851–1865, 2001.
- Vogels R, Spileers W, and Orban GA.** The response variability of striate cortical neurons in the behaving monkey. *Exp Brain Res* 77: 432–436, 1989.
- Warzecha AK and Egelhaaf M.** Variability in spike trains during constant and dynamic stimulation. *Science* 283: 1927–1930, 1999.
- Warzecha AK, Kretzberg J, and Egelhaaf M.** Reliability of a fly motion-sensitive neuron depends on stimulus parameters. *J Neurosci* 20: 8886–8896, 2000.
- Zaagman WH, Mastebroek HAK, and de Ruyter van Steveninck R.** Adaptive strategies in fly vision: on their image-processing qualities. *IEEE Trans Syst Man Cybern* 5: 900–906, 1983.